

Failure investigation of a Kaplan turbine blade

Ming Zhang

David Valentin*

david.valentin@upc.edu

Carme Valero

Mònica Egusquiza

Eduard Egusquiza

Center for Industrial Diagnostics and Fluid Dynamics (CDIF), Polytechnic University of Catalonia (UPC), Av. Diagonal, 647, ETSEIB, 08028 Barcelona, Spain

*Corresponding author.

Abstract

In this paper, an uncommon failure of a Kaplan turbine blade has been analyzed. After the monitoring system detected a sudden increase in vibration levels, the turbine was inspected. The inspection showed that a large crack occurred on one blade starting from the leading-edge side root hole. Moreover, the tip of the blade was also found broken. A comprehensive analysis of the crack surfaces, broken parts and the vibration data revealed a fatigue problem probably caused by rubbing between the blade and the nearby wall.

The effect of contacts on the stress distribution of the blade was investigated through a numerical model of the turbine blade. To validate this numerical model an experimental modal analysis was done on a non-damaged blade and the results showed a good agreement with the numerical results. Stress distribution analysis showed that when applying a contact force, the stress at the leading-edge root hole increases drastically. Therefore, experimental evidences as well as numerical simulations confirm that the crack occurred due to rubbing between the blade tip and the nearby wall.

1.1 Introduction

Kaplan turbines are widely used in low water head and large capacity hydropower plants due to their good performance in their whole range of operation [1]. The runner of Kaplan turbines consists of several blades that can change their incidence flow angle in order to ensure good performance for all the operating points. This angle is changed by means of a complex control system located inside the hub and shaft (see Fig. 1). Moreover, there is a narrow gap between the blade tips and the nearby stationary wall, which is commonly named as tip clearance. In order to ensure a good performance of the machine, this tip clearance has to be very small, normally of about 0.05% the runner diameter. Details of a typical Kaplan turbine are shown in Fig. 1.

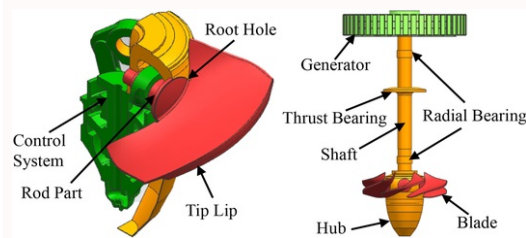


Fig. 1. Fig. 1 Kaplan turbine assembly.

alt-text: Fig. 1

Typical damage types in Kaplan turbine are caused by silt erosion [2,3], cavitation [4-6] and fatigue [7-10]. Erosion usually affects the surface of the blades, due to the high velocities of the water, and it is expected to appear in

areas where the water has suspended particles [2,3]. Cavitation may occur in Kaplan turbines because of an improper blade profile or extreme off-design operation conditions [4,5]. One common type of cavitation is the tip clearance cavitation, which appears in the gap between the blade tip and the stationary nearby wall [5]. One way of avoiding this cavitation type is to reduce the tip clearance to its technological minimum, which increases the chances of having rubbing between the blade tip and the wall. Another method of dealing with this cavitation type is to install the so-called anti-cavitation tip-lips (see Fig.1). However, most of the cases of damage in Kaplan turbines come from fatigue problems [11].

Kaplan turbines are subjected to both static and dynamic pressure loads. The static pressure load is proportional to the net head and the flow rate passing through the runner. The dynamic pressure load is caused by the Rotor Stator Interaction (RSI) [12,13] or other and less common dynamic phenomena such as vortex rope, tip vortex and Von Karman vortices [11,13-15]. Some studies [9,12] have shown that the water pressure load can induce high-stress concentration at the root area of the blade and on the piston rod as shown in some references [7, 10, 16]. Some of these studies presented also cases of resonances, where the frequencies of the runner coincided with the dynamic pressure excitation frequencies, increasing drastically the blade vibration, and therefore causing severe damage to the blade. Moreover, if the material has defects at this zone, the fatigue process can be greatly accelerated.

Another case of damage in Kaplan turbines, but less common, is rubbing. Due to the small tip clearance, the blade tip may contact the stationary wall due to high radial forces, normally caused by unbalance or fluid instabilities [17]. Unbalance can be of mechanical or hydraulic origin. Mechanical unbalance could be induced by a non-correct assembly of the rotating train, especially of the runner blades or the generator poles, a failure in the bearings, a loss of stiffness of the machine supports or other problems associated to a non-distributed rotating mass. Hydraulic unbalance in Kaplan turbines could occur when the flow present asymmetric characteristics, such as under rough operating conditions with the appearance of cavitation or vortex rope. Rubbing in rotating machines is known to produce high impact forces and can lead to catastrophic failures in the worst-case scenario [18]. Thiery et al. [17] performed some theoretical analysis about blade tip-wall contacts. They introduced some parameters to study the problem, like the contact stiffness or damping. Results showed that, under rotation, if the contact frequency (times that the blades contact the wall per revolution) is near a natural frequency of the rotor, the vibration of the shaft could be amplified drastically, increasing also the strength of the contact. However, this study is only theoretical, there are no failure cases of prototype Kaplan turbines due to rubbing available in the literature.

In this paper, an uncommon failure of a Kaplan turbine blade due to rubbing has been analyzed. After the monitoring system detected a sudden increase in vibration levels, the machine was stopped and inspected. The inspection of the turbine showed that a large crack occurred on one blade starting from the leading-edge side root hole. Moreover, the tip-lip of the blade was also found broken. A comprehensive analysis of the crack surfaces, broken tip-lip and the vibration data revealed a fatigue problem probably caused by rubbing between the damaged blade and the nearby wall. To demonstrate this theory, a numerical blade model was used. First, this numerical model was validated by an experimental modal analysis. Then, the pressure due to the water load was applied and, finally a contact force was introduced in the model. Results showed an increase in the stress in the part where the crack started. Therefore, both experimental and numerical evidences demonstrate that the crack appeared in the blade due to rubbing between the blade tip and the stationary wall.

2.2 Damage description

The case reported in this paper corresponds to a Kaplan turbine with a head of 34 m and maximum power of 73 MW. It is a vertical machine supported by a thrust bearing in the lower side of the generator, and two radial bearings, one in the turbine side and another in the generator side. The runner has 6 blades rotating at 125 rpm and the distributor has 24 guide vanes. The tip clearance is of 0.09% the outlet diameter of the runner.

Periodically, vibration monitoring is carried out to supervise the condition of the turbine. This procedure consists of measuring the vibration on some accessible points of the machine allowing the detection of abnormal vibrational behavior and, in some cases, incipient damage. For this case, data was measured in the bearings in axial and radial directions. In one of the measurements, the vibration monitoring system detected an increase in the overall vibration levels, as well as a clear change in the spectra obtained by performing the Fast Fourier Transform (FFT) of the time signal. Therefore, the machine was stopped and inspected.

The inspection of the runner showed a large crack starting from the leading-edge side root hole of one of the blades (Fig. 2). A detail of the crack is seen in Fig. 3, where the beach marks can be also discerned. The beach marks show that the damage was caused by a fatigue problem. In addition, some scratches were found on the whole perimeter of the stationary wall and the tip-lip of the damaged blade was also found broken (see Fig. 4 and Fig. 5). This fact leads one to think that a contact between the tip-lip of the blade and the wall occurred. To better understand how the blade was broken, a further investigation using a numerical blade model is carried out in the following sections.

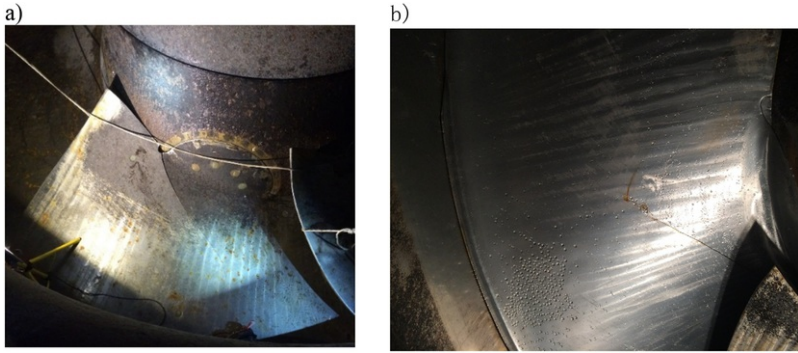


Fig. 2 View of the blade with crack. a) Pressure side. b) Suction side.

alt-text: Fig. 2

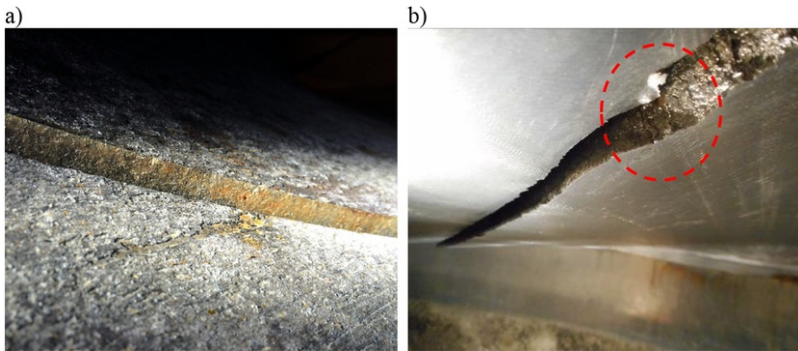


Fig. 3 Detail of the crack. a) From the pressure side. b) From the suction side.

alt-text: Fig. 3

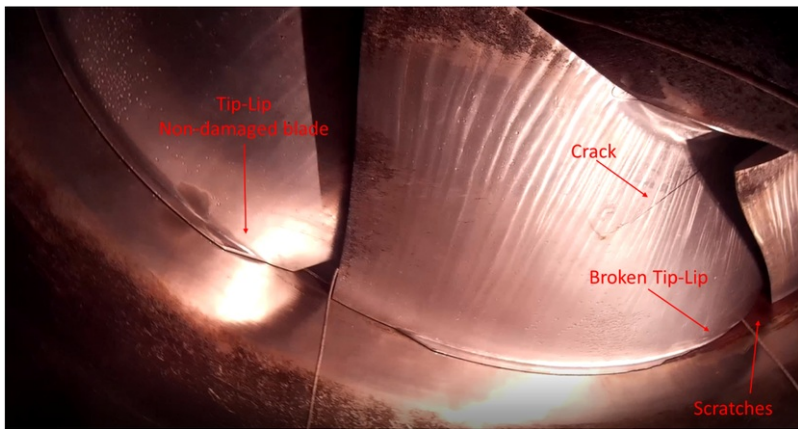


Fig. 4 View of the runner from below. Non-damaged blade (left) and damaged blade (right).

alt-text: Fig. 4

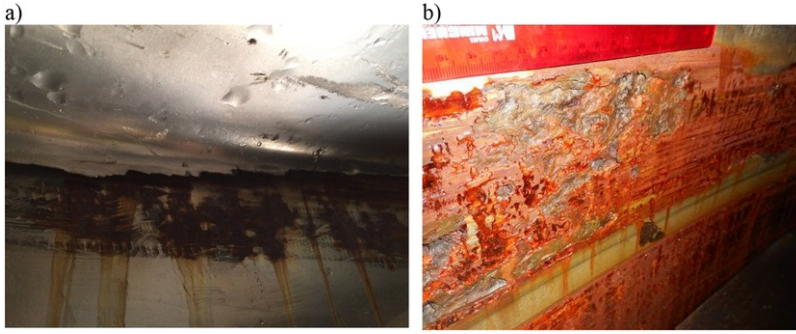


Fig. 5. Detail of the broken tip-lip and scratches in the stationary wall. a) Detail of the broken tip-lip. b) Detail of the scratches in the wall.

alt-text: Fig. 5

3.3 Analysis of the machine vibration

As mentioned above, the machine was monitored periodically by analyzing vibration in the bearings. Analyzing the vibration overall levels as well as the spectra of every measured point, the status of the machine can be evaluated [19-21]. However, first, it is essential to understand the origin of the vibration in the turbine.

Vibrations generated by Kaplan turbines can be of mechanical origin or of hydraulic origin. Mechanical origin forces are mainly the centrifugal forces, which depend on the distribution of the rotating mass and on the rotational speed. The hydraulic forces can be divided in two types: the static loads and the hydrodynamic loads. The static load is caused by the mas-flow passing through the runner and therefore they are higher for higher generating powers [12]. The hydrodynamic loads mainly come due to the Rotor Stator Interaction (RSI), although they can also provide from other hydraulic phenomena such as vortex rope, tip vortex or Vortex-shedding [14,15,22-24].

The RSI arises from the interference between the rotating blades of the runner and the stationary guide vanes [25]. In Kaplan turbines, RSI is not as important as in Francis turbines or Pump-turbines, but it still exists. Viewed from the stationary frame, the RSI frequency depend on the rotating speed of the runner (f_r), the number of rotating blades (Z_b) and the order of harmonics (n):

$$f_{b,n} = n \cdot Z_b \cdot f_r \tag{1}$$

The excitation shape corresponding every $f_{b,n}$ is the superposition of several excitation modes (k) that can be calculated with the following expression:

$$k = m \cdot Z_v - n \cdot Z_b \tag{2}$$

where Z_v is the number of guide vanes and m the order of harmonics from the rotating view. The highest amplitudes are obtained for the minimum values of $|k|$. For this case, the combination of m and n that minimizes $|k|$ is $m = 1$ and $n = 4$, being $k = 0$. The sign of k indicates the rotation of the pressure pulsation. If it is positive the pressure pulsation rotates in the same direction than the runner and if it is negative, it rotates in the opposite direction.

Fig. 6(a) shows a typical vibration signature of a Kaplan turbine in a turbine bearing without any damage. The vibration signature for the generator bearing without any damage is seen in Fig. 7(a). Three peaks can be clearly identified: f_r , $f_{b,2}$ and $f_{b,4}$. However, a sudden increase in the harmonics related with the f_r was found when the blade was broken (see Fig. 6(b) and Fig. 7(b)). The unbalance, related with the f_r increased considerably in comparison with the one with the machine in good condition (Fig. 6(a) and Fig. 7(a)). These symptoms coincide with a severe unbalanced rotating machine and with a blade contacting in the stationary wall during operation, which would induce one strong impact to the blade every revolution, exciting also the natural frequencies of the system.

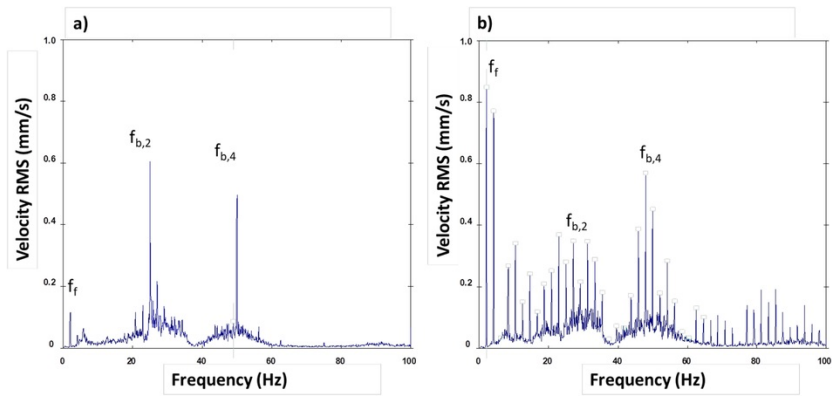


Fig. 6. Fig. 6 Comparison between the spectra before damage (a) and with damage (b). Turbine bearing.

alt-text: Fig. 6

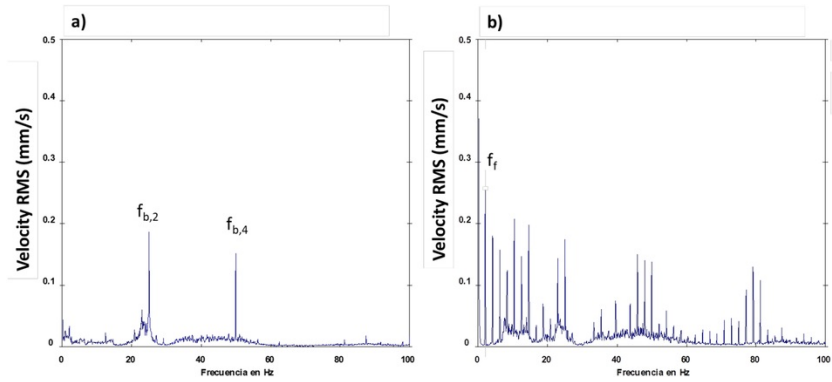


Fig. 7. Fig. 7 Comparison between the spectra before damage (a) and with damage (b). Generator bearing.

alt-text: Fig. 7

The overall vibration levels of all the measured points also increased considerably. Fig. 8 shows these levels for the turbine bearing and the generator bearing. After the reparation of the blade, the symptoms observed with the broken blade disappeared.

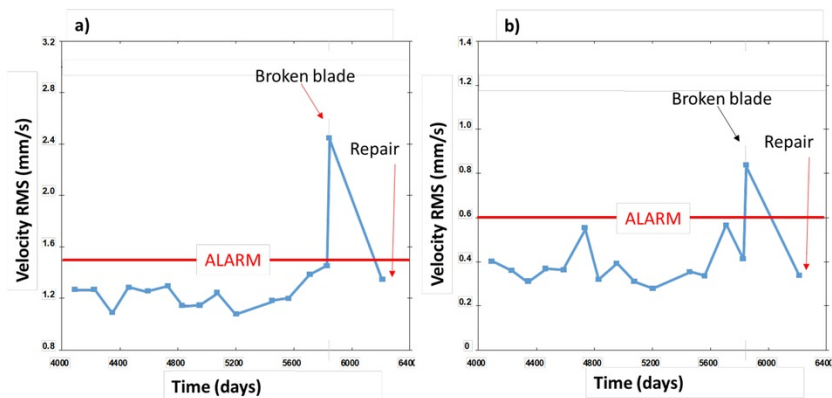


Fig. 8, Fig. 8 Overall vibration levels along the time. a) Turbine bearing. b) Generator bearing.

alt-text: Fig. 8

4.4 Numerical simulation

A numerical model of one blade has been built up in order to simulate the stress distribution in the blade. This numerical model considers the rod, the blade and the tip-lip (see Fig. 9). Ansys Workbench 17 [26] has been used to solve all the simulations in this paper. The material used in the simulation is stainless steel (density of 7750 kg/m^3 , Young's Modulus of 193 GPa and Poisson's ratio of 0.31). The blade is fixed at the rod using a totally fixed support. The mesh sensitivity was strictly checked and the mesh density at the root holes, which are the typical stress concentrator points, was especially increased. Finally, about $1.4 \cdot 10^5$ tetrahedral elements were used, as shown in Fig. 9.

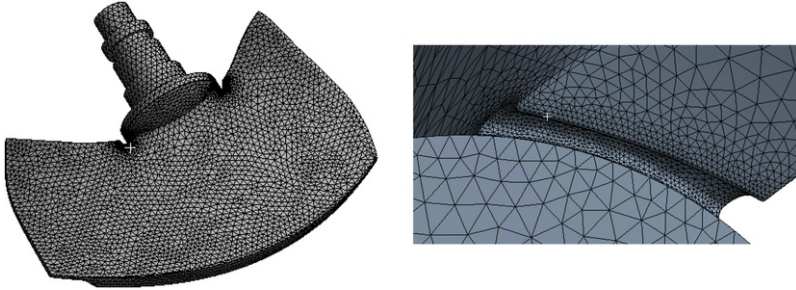


Fig. 9, Fig. 9 View of the mesh.

alt-text: Fig. 9

First, a modal analysis was performed and the results were compared with experimental values (see Section 5). Once the numerical model was validated, the typical static pressure distribution over a Kaplan blade was applied in the model. This pressure distribution was applied according to the reference [14] (see Fig. 10(a)). In this reference, the pressure distribution was obtained by CFD (Computational Fluid Dynamics). The static pressure distribution in Kaplan blades depends on the operating point because the blades present different angle for every flow rate. In this case, the pressure distribution used corresponds to 67% of guide vane opening, which is a point slightly below the BEP (Best Efficiency Point). The rotating speed was also introduced to the blade to consider the inertia effects. The stress distribution was obtained for this pressure distribution. After that, one tangential force and one radial force were applied in the blade tip, just were it was found broken in the prototype (see Fig. 10(b)). These forces model the behavior of a contact with the stationary wall. As the value of these forces was not known, different values were tested to see the influence of those forces on the stress distribution over the blade.

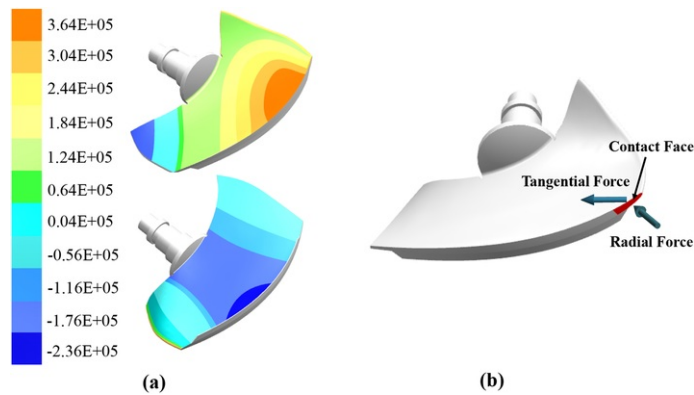


Fig. 10, Fig. 10 Pressure pattern (unit: Pa). b) Contact forces.

alt-text: Fig. 10

5.5 Experimental modal analysis

To validate the numerical model, an Experimental Modal Analysis (EMA) [27-29] was done. De Souza Braga et al. [30] studied the modal behavior of an axial flow turbine numerically and experimentally. The results showed that the blades' mode-shapes are not affected between each other, therefore the modal behavior of the whole runner can be represented by the modal behavior of a single blade.

5.1.5.1 Set-up and instrumentation

The EMA was done on a non-damaged blade of the runner, as shown in Fig. 11. The blade was impacted using an instrumented hammer (Dytran 5802A, 220 $\mu\text{V}/\text{N}$) and the response was measured using an accelerometer (Kistler 8752A, 100 mV/g). Both accelerometer and sensor were connected to a Bruel & Kjaer (LAN XI Type 3053) acquisition system which recorded the signals in the time domain. The blade was impacted always in the same point (see Fig. 11) and the accelerometer was moved to 21 different positions in order to represent the mode-shape of the blade for every natural frequency. This method is called roving accelerometer [27,28]. Three impacts were done in every position of the accelerometer in order to compute the average of them. The positions where the accelerometer was placed are shown in Fig. 11.

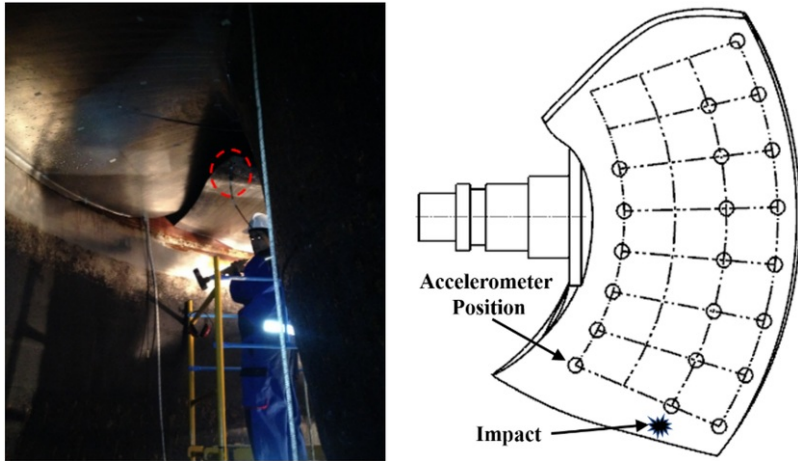


Fig. 11. Experimental Modal Analysis. Not include the radius, not necessary.

alt-text: Fig. 11

5.2.5.2 Signal analysis

To analyze every point, a frequency response function (FRF) between the accelerometers and the hammer was computed. The average in a frequency domain of three impacts was used taking 8 s of time signal and a frequency resolution of 0.125 Hz (400 Hz maximum frequency analyzed). The coherence function was also computed between the accelerometer and the hammer in order to ensure the accuracy of the experimental testing. In that way, one FRF was obtained for every point where the accelerometer was located (21 in total). Using the 21 FRFs, an operational deflection shape (ODS) [28,31] of the runner can be obtained.

5.3.5.3 Natural frequencies and mode-shapes

A FRF of one of the points analyzed is shown in Fig. 12. The first five natural frequencies of the blade are observed between 0 and 200 Hz. The mode-shapes associated to every of those natural frequencies are shown in Table 1 and in supplementary videos. In this table, the results obtained by simulation are also shown. It is seen that there is a good agreement between experiment and simulation since both mode-shapes and values of natural frequencies are very close.

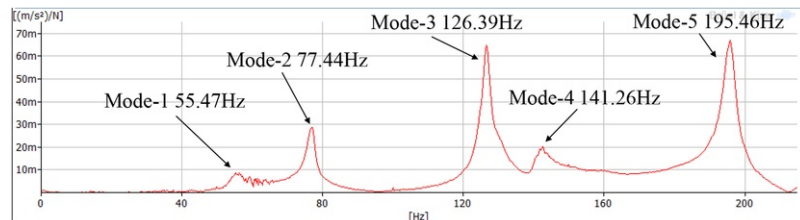
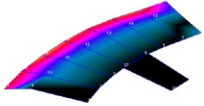
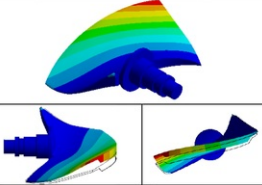
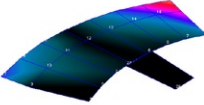
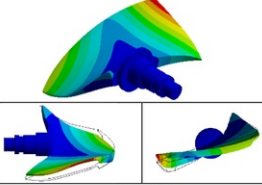
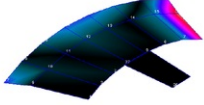
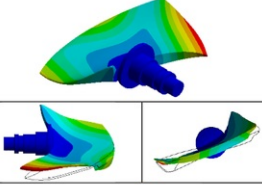
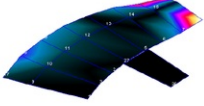
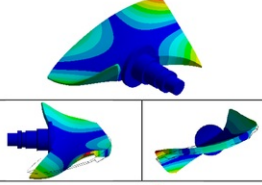
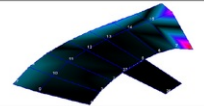
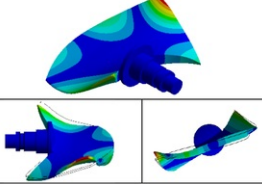
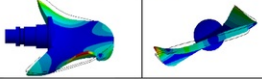


Fig. 12. Frequency Response Function. Change mode-shapes names by Mode 1, Mode 2, Mode 3, Mode 4, Mode 5.

alt-text: Fig. 12

Table 1. Experimental and numerical modes. Mode-shapes animations added as supplementary material.

Mode	Experimental Results		Numerical Results		
	Freq [Hz]	Modal Shape	Freq [Hz]	Modal Shape	
Mode-1	55.47		61.83		
Mode-2	77.44		70.53		
Mode-3	126.39		103.08		
Mode-4	141.26		142.39		
Mode-5	195.46		186.97		
					

alt-text: Table 1

6.6 Dynamic response of the blade

To determine the effect of rubbing on the stress distribution of the blade and its relationship with the crack appearance, a static structure analysis of the blade was performed. To do so, first, a typical pressure distribution in Kaplan turbines is applied to the structure as explained in [Section 4](#) and then, a contact force was applied in the tip of the blade.

6.1.6.1 Stress distribution under normal operating conditions

Once the pressure pattern over the blade is applied, the stress distribution due to this pressure is obtained. Therefore, this stress distribution corresponds to the normal operating conditions of the machine and it is shown in Fig. 13(a). The displacement of the blade is also shown in Fig. 13(b). It is observed that the maximum stress in the blade is located in the zone where the crack started in the machine. The stress distribution matches with other previously obtained in other Kaplan turbine prototypes [12].

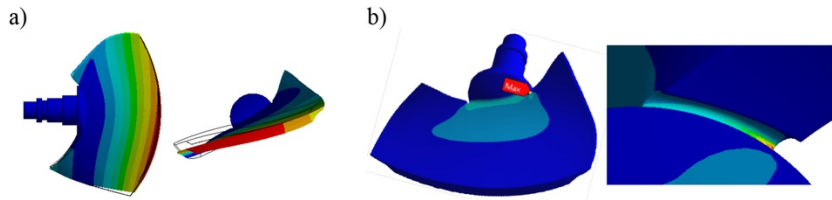


Fig. 13. Fig. 13 a) Displacement of the blade under normal operating conditions. b) Stress distribution under normal operating conditions.

alt-text: Fig. 13

6.2.6.2 Stress distribution with rubbing

To model the rubbing, a radial force and a tangential force were applied to the blade (see Fig. 10(b)). The value of these forces is not known, hence different values were tested in the simulation. Fig. 14 shows how the value of these forces affect the maximum stress value located in the root of the blade, where the crack started. The figure shows the stress normalized against the value found without any rubbing (Section 6.1). It is seen that for the contact forces from 10^6N to 10^7N , the stress value increases drastically. From the case of the scratched wall and broken tip-lip, the contact force in this researched case ought to be very high. Therefore, with the appearance of these tangential and radial forces the stress in the root increases and it demonstrates the appearance of the crack in the blade.

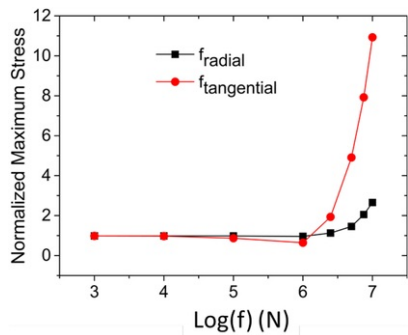


Fig. 14. Fig. 14 Normalized maximum stress changes with contact force.

alt-text: Fig. 14

However, not only the stress in this point increases, but also the stress distribution changes due to the appearance of a tangential and radial force in the blade tip. Fig. 15 shows the displacement and stress distribution due to different values of tangential and radial forces. It can be observed that the stress is also higher in the zone of the tip-lip, just where it was also found broken. This fact demonstrates why this part was also found broken in the machine inspection.

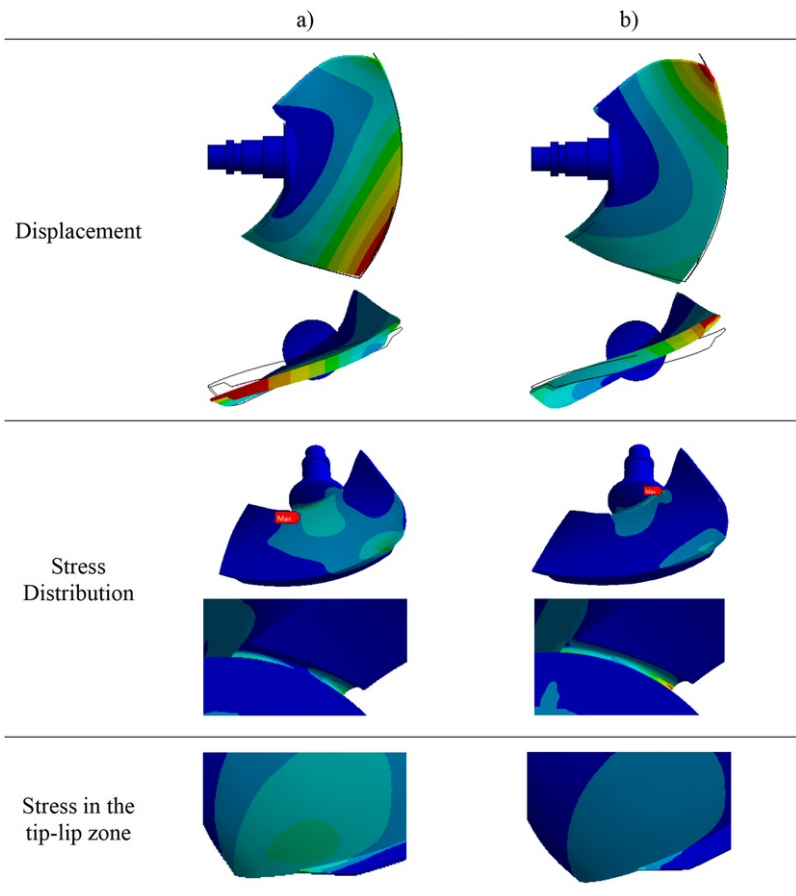


Fig. 15. Fig. 15 Displacement and stress distribution a) Tangential force value of 10^6N . b) Radial force value of 10^7N .

alt-text: Fig. 15

7.7 Conclusions

In this paper, an uncommon failure of a Kaplan turbine blade has been analyzed to find out the causes that provoked it.

Kaplan turbine blades are prone to have fatigue problems due to high hydraulic loads. The root area is usually the high-stress area and is easy for the crack to initiate. In the present case, a large crack occurred on one blade starting from the leading-edge side root hole. This damage generated an increase in the vibrations of the machine that was detected by the monitoring system.

After inspection, beach marks were found on the crack surfaces, which indicated that the crack was caused by fatigue. At the same time, some scratches were found on the chamber wall and the tip-lip near the leading-edge was broken. This showed that there had been a contact between the damaged blade and the wall.

To research the effect of the contact on the stress distribution of the blade and its relationship with crack appearance, static structure analysis was done. To validate the numerical model used for static structure analysis, experimental modal analysis was done on an intact blade and the results showed that both the modes and their appearance sequences had good agreements with the numerical results.

For static structure analysis, the hydraulic pressures on the pressure and suction sides from the literature as well as the centrifugal force due to the rotation were implemented together. The results showed that with the increase of the contact force, the stress at the leading-edge root hole increases drastically. A high-stress area also appeared at the tip-lip zone. Therefore, it ought to be the high contact force that caused the crack and broken tip-lip to

occur.

Supplementary data to this article can be found online at <https://doi.org/10.1016/j.engfailanal.2019.01.056>.

Acknowledgements

The author wishes to acknowledge the contribution of ENDESA team to the development of this paper.

References

- [1] E.E. Estevez, Comportament dinàmic de màquines hidràuliques, 2004, Univ. Politèc. de Catalunya.
- [2] M.K. Padhy and R.P. Saini, A review on silt erosion in hydro turbines, *Renew. Sustain. Energy Rev.* **12**, 2008, 1974–1987.
- [3] D. Kumar and P.P. Bhingole, CFD based analysis of combined effect of cavitation and silt erosion on Kaplan turbine, *Mater. Today Proc.* **2**, 2015, 2314–2322.
- [4] X. Escaler, E. Egusquiza, M. Farhat, F. Avellan and M. Coussirat, Detection of cavitation in hydraulic turbines, *Mech. Syst. Signal Process.* **20**, 2006, 983–1007, <https://doi.org/10.1016/j.ymsp.2004.08.006>.
- [5] L. Motycak, A. Skotak and R. Kupcik, Kaplan turbine tip vortex cavitation—analysis and prevention, In: *IOP Conf. Ser. Earth Environ. Sci.*, 2012, 32060.
- [6] P. Kumar and R.P. Saini, Study of cavitation in hydro turbines—A review, *Renew. Sustain. Energy Rev.* **14**, 2010, 374–383, <https://doi.org/10.1016/j.rser.2009.07.024>.
- [7] Z.W. Wang, Y.Y. Luo, L.J. Zhou, R.F. Xiao and G.J. Peng, Computation of dynamic stresses in piston rods caused by unsteady hydraulic loads, *Eng. Fail. Anal.* **15**, 2008, 28–37.
- [8] G. Urquiza, J.C. Garcia, J.G. Gonzalez, L. Castro, J.A. Rodriguez, M.A. Basurto-Pensado and O.F. Mendoza, Failure analysis of a hydraulic Kaplan turbine shaft, *Eng. Fail. Anal.* **41**, 2014, 108–117.
- [9] D. Frunzaverde, V. Campian, D. Nedelcu, G.-R. Gillich and G. Marginean, Failure analysis of a kaplan turbine runner blade by metallographic and numerical methods, In: *Proc. 7th WSEAS Int. Conf. FLUID Mech. (FLUIDS'10)*, 2010, Univ. Cambridge, UK, 60–67.
- [10] Y. Luo, Z. Wang, J. Zeng and J. Lin, Fatigue of piston rod caused by unsteady, unbalanced, unsynchronized blade torques in a Kaplan turbine, *Eng. Fail. Anal.* **17**, 2010, 192–199.
- [11] X. Liu, Y. Luo and Z. Wang, A review on fatigue damage mechanism in hydro turbines, *Renew. Sustain. Energy Rev.* **54**, 2016, 1–14.
- [12] L. Zhou, Z. Wang, R. Xiao and Y. Luo, Analysis of dynamic stresses in Kaplan turbine blades, *Eng. Comput.* **24**, 2007, 753–762.
- [13] S. Liu, S. Li and Y. Wu, Pressure fluctuation prediction of a model Kaplan turbine by unsteady turbulent flow simulation, *J. Fluids Eng.* **131**, 2009, 101102.
- [14] Y. Wu, S. Liu, H.-S. Dou, S. Wu and T. Chen, Numerical prediction and similarity study of pressure fluctuation in a prototype Kaplan turbine and the model turbine, *Comput. Fluids.* **56**, 2012, 128–142.
- [15] L. Motycak, A. Skotak and J. Obrovsky, Analysis of the Kaplan turbine draft tube effect, In: *IOP Conf. Ser. Earth Environ. Sci.*, 2010, 12038.
- [16] X. Liu, A. Presas, Y. Luo and Z. Wang, Crack growth analysis and fatigue life estimation in the piston rod of a Kaplan hydro turbine, *Fatigue Fract. Eng. Mater. Struct.* 2018.
- [17] F. Thiery, R. Gustavsson and J.-O. Aidanpää, Dynamics of a misaligned Kaplan turbine with blade-to-stator contacts, *Int. J. Mech. Sci.* **99**, 2015, 251–261.
- [18] G. Jacquet-Richardet, M. Torkhani, P. Cartraud, F. Thouverez, T. Nouri Baranger, M. Herran, C. Gibert, S. Baguet, P. Almeida and L. Peletan, Rotor to stator contacts in turbomachines. Review and application, *Mech. Syst. Signal Process.* **40**, 2013, 401–420, <https://doi.org/10.1016/j.ymsp.2013.05.010>.
- [19] E. Egusquiza, C. Valero, D. Valentin, A. Presas and C.G. Rodriguez, Condition monitoring of pump-turbines. New challenges, *Meas. J. Int. Meas. Confed.* 2015, <https://doi.org/10.1016/j.measurement.2015.01.004>.
- [20] M. Egusquiza, E. Egusquiza, C. Valero, A. Presas, D. Valentin and M. Bossio, Advanced condition monitoring of Pelton turbines, *Measurement* **119**, 2018, 46–55, <https://doi.org/10.1016/j.measurement.2018.01.030>.
- [21] A. Presas, D. Valentin, M. Egusquiza, C. Valero, E. Egusquiza, A. Presas, D. Valentin, M. Egusquiza, C. Valero and E. Egusquiza, Sensor-Based optimized control of the full load instability in large hydraulic turbines,

[Sensors](https://doi.org/10.3390/s18041038), **18**, 2018, 1038, <https://doi.org/10.3390/s18041038>.

- [22] B.G. Mulu, P.P. Jonsson and M.J. Cervantes, Experimental investigation of a Kaplan draft tube--Part I: Best efficiency point, *Appl. Energy* **93**, 2012, 695-706.
- [23] P.P. Jonsson, B.G. Mulu and M.J. Cervantes, Experimental investigation of a Kaplan draft tube--Part II: off-design conditions, *Appl. Energy* **94**, 2012, 71-83.
- [24] K. Amiri, B. Mulu, M. Raisee and M.J. Cervantes, Load variation effects on the pressure fluctuations exerted on a Kaplan turbine runner, In: *IOP Conf. Ser. Earth Environ. Sci.* 2014, 32005.
- [25] C.G. Rodriguez, E. Egusquiza and I.F. Santos, Frequencies in the vibration induced by the rotor stator interaction in a centrifugal pump turbine, *J. Fluids Eng.* **129**, 2007, 1428-1435, <https://doi.org/10.1115/1.2786489>
- [26] ANSYS(R), Ansys User's Manual 17.0, Canonsburg, Pennsylvania, USA 2017.
- [27] P. Avitabile, Experimental modal analysis, *Sound Vib.* **35**, 2001, 20-31.
- [28] D. Valentin, A. Presas, M. Bossio, M. Egusquiza, E. Egusquiza and C. Valero, feasibility of detecting natural frequencies of hydraulic turbines while in operation, using strain gauges, *Sensors* **18**, 2018, 174.
- [29] A. Presas, D. Valentin, E. Egusquiza, C. Valero, M. Egusquiza and M. Bossio, Accurate determination of the frequency response function of submerged and confined structures by using PZT-patches, *Sensors* 2017, <https://doi.org/10.3390/s17030660>, (Switzerland).
- [30] D. de Souza Braga, D.F. Coelho, N.S. Soeiro, G. da S.V. de Melo and A.L.A. Mesquita, Numerical simulation of fluid added mass effect on a Kaplan turbine runner with experimental validation, In: *22nd Int. Congr. Mech. Eng. (COBEM 2013)*, 2013, 4331-4339.
- [31] B.J. Schwarz and M.H. Richardson, Introduction to operating deflection shapes, *CSI Reliab. Week.* **10**, 1999, 121-126.

[The following are the supplementary data related to this article.](#)

[Multimedia Component 1](#) 

Supplementary video S1

alt-text: Supplementary video S1

[Multimedia Component 2](#) 

Supplementary video S2

alt-text: Supplementary video S2

[Multimedia Component 3](#) 

Supplementary video S3

alt-text: Supplementary video S3

[Multimedia Component 4](#) 

Supplementary video S4

alt-text: Supplementary video S4

[Multimedia Component 5](#) 

Supplementary video S5

alt-text: Supplementary video S5

[Multimedia Component 6](#)



Supplementary video S6

alt-text: Supplementary video S6

[Multimedia Component 7](#)



Supplementary video S7

alt-text: Supplementary video S7

[Multimedia Component 8](#)



Supplementary video S8

alt-text: Supplementary video S8

[Multimedia Component 9](#)



Supplementary video S9

alt-text: Supplementary video S9

[Multimedia Component 10](#)



Supplementary video S10

alt-text: Supplementary video S10

Highlights

- A large crack was discovered in a Kaplan turbine blade.
- A failure investigation of the crack was performed.
- Experimental research on the dynamic behavior of a Kaplan turbine blades was carried out.
- A numerical model of the Kaplan turbine blade was validated and used for studying the origin of the crack.
- Rubbing between the blade and the stationary wall was demonstrated to be the cause of the crack appearance.

Queries and Answers

Query:

Your article is registered as a regular item and is being processed for inclusion in a regular issue of the journal. If this is NOT correct and your article belongs to a Special Issue/Collection please contact s.sadhasivan@elsevier.com immediately prior to returning your corrections.

Answer: Yes

Query:

Please confirm that given names and surnames have been identified correctly and are presented in the desired order, and please carefully verify the spelling of all authors' names.

Answer: Yes

Query:

The author names have been tagged as given names and surnames (surnames are highlighted in teal color). Please confirm if they have been identified correctly.

Answer: Yes

Query:

Please check whether the designated corresponding author is correct, and amend if necessary.

Answer: Correct

Query:

Please provide caption for Supplementary video S1.

Answer: Mode 1. Experimental

Query:

Please provide caption for Supplementary video S2.

Answer: Mode 2. Experimental

Query:

Please provide caption for Supplementary video S3.

Answer: Mode 3. Experimental

Query:

Please provide caption for Supplementary video S4.

Answer: Mode 4. Experimental

Query:

Please provide caption for Supplementary video S5.

Answer: Mode 5. Experimental

Query:

Please provide caption for Supplementary video S6.

Answer: Mode 1. Numerical Simulation

Query:

Please provide caption for Supplementary video S7.

Answer: Mode 2. Numerical Simulation

Query:

Please provide caption for Supplementary video S8.

Answer: Mode 3. Numerical Simulation

Query:

Please provide caption for Supplementary video S9.

Answer: Mode 4. Numerical Simulation

Query:

Please provide caption for Supplementary video S10.

Answer: Mode 5. Numerical Simulation

Query:

Correctly acknowledging the primary funders and grant IDs of your research is important to ensure compliance with funder policies. We could not find any acknowledgement of funding sources in your text. Is this correct?

Answer: Yes

Query:

Please provide the volume number and page range for the bibliography in Ref. [16].

Answer: Volume 41, Issue 11, pages 2402-2417